



Published in final edited form as:

J Orthop Res. 2020 January ; 38(1): 43–58. doi:10.1002/jor.24448.

Transcriptomic Analysis of Cellular Pathways in Healing Flexor Tendons of Plasminogen Activator Inhibitor 1 (PAI-1/Serpine1) Null Mice

Margaret A. T. Freeberg^{1,2}, Anas Easa², Jacquelyn A. Lillis⁴, Danielle S.W. Benoit^{1,2}, Andre J. van Wijnen⁵, Hani A. Awad^{1,2,3}

¹Department of Biomedical Engineering, University of Rochester, Rochester, NY, United States

²Center for Musculoskeletal Research, University of Rochester, Rochester, NY, United States

³Department of Orthopedics, University of Rochester, Rochester, NY, United States

⁴Genomics Research Center, University of Rochester, Rochester, NY, United States

⁵Orthopedic Surgery, Mayo Clinic, Rochester, MN, United States

Abstract

Injuries to flexor tendons can be complicated by fibrotic adhesions, which severely impair the function of the hand. Plasminogen Activator Inhibitor 1 (PAI-1/SERPINE1), a master suppressor of fibrinolysis and protease activity, is associated with adhesions. Here, we used next-generation RNA sequencing (RNA-Seq) to assess genome-wide differences in mRNA expression due to PAI-1 deficiency after zone II flexor tendon injury. We used Ingenuity Pathway Analysis to characterize molecular pathways and biological drivers associated with differentially expressed genes. Analysis of hundreds of overlapping and differentially-expressed genes in PAI-1 knockout (KO) and wild type mice (C57Bl/6J) during tendon healing revealed common and distinct biological processes. Pathway analysis identified cell proliferation, survival, and senescence, as well as chronic inflammation as potential drivers of fibrotic healing and adhesions in injured tendons. Importantly, we identified the activation of PTEN signaling and the inhibition of FOXO1-associated biological processes as unique transcriptional signatures of the healing tendon in the PAI-1/Serpine1 KO mice. Further, transcriptomic differences due to the genetic deletion of PAI-1 were mechanistically linked to PI3K/Akt/mTOR, PKC, and MAPK signaling cascades. These

Corresponding Author Hani A. Awad, Ph.D., University of Rochester Medical Center, 601 Elmwood Avenue, Box 665, Rochester, NY 14642, United States, Phone: 1-585-273-5268, Fax: 1-585-276-2177, hani_awad@urmc.rochester.edu.

Author Contributions

Conceptualization, HA, AV, MTF;

Methodology, MTF, AE, JL, HA;

Software, MTF, JL, HA;

Formal Analysis, MTF, HA;

Investigation, MTF, AE;

Writing – Original draft, MTF, HA;

Writing – Reviewing & Editing, MTF, AE, JL, AV, DB, HA;

Visualization, MTF, HA;

Supervision, DB, HA;

Project Administration, HA, DB;

Funding Acquisition, HA, DB;

Competing financial interests

The authors declare no competing financial interests.

transcriptional observations provide novel insights into the biological roles of PAI-1 in tendon healing and therapeutic targets to achieve scar-free regenerative healing of tendons.

Keywords

RNA sequencing; Ingenuity Pathway Analysis; Tendon; Adhesions; Fibrosis; PAI-1; PTEN; FOXO1

Introduction

Injuries to flexor tendons in zone II of the hand often lead to poor healing outcomes. Restoration of function after surgical repair can be impaired due to the formation of scar tissue adhesions and the incidence of tendon re-rupture, often necessitating additional surgery ¹. The complexities of cellular and biological mechanisms that mediate optimal tendon healing, or that lead to adhesions and inferior tissue biomechanics, are not fully appreciated. This gap in knowledge is a significant barrier to the development of clinically translatable biological therapies to improve the outcomes of tendon healing. To address this, gain- or loss-of-function approaches using genetic mouse models are increasingly used in preclinical studies of tendon injury to investigate the functional contributions of specific genes in hypothesized mechanisms of scar-mediated healing.

We have previously shown that the pleiotropic protease suppressor, Plasminogen Activator Inhibitor 1 or PAI-1, is ubiquitously secreted in the extracellular matrix of scar tissue in injured flexor tendons of C57Bl/6J mice. Incidentally, elevated levels of PAI-1 were also observed in fibrotic flexor tendon tissue of Dupuytren's contracture hands ². Further, PAI-1 polymorphisms are predisposing factors to post-operative adhesions following general surgery ³. Given its well-described roles in fibrosis in a variety of tissues and organs ⁴, it has been shown that PAI-1 not only inhibits fibrinolysis leading to aberrant persistence of provisional fibrin matrix in the early stages of healing and a delay in the resolution of inflammation but also inhibits plasmin-mediated activation of matrix metalloproteases (MMPs). The reduced activity of MMPs slows the remodeling of scar tissue, which we hypothesized precipitates flexor tendon adhesions. In concordance with this hypothesis, we have shown that zone II flexor tendon healing in PAI-1 knockout (KO) mice exhibits reduced adhesion formation and accelerated the reestablishment of injured tendon mechanical properties compared to wild type C57Bl/6J mice ². Based on these findings, PAI-1 has been identified as a therapeutic target for the treatment of flexor tendon fibrotic adhesions.

PAI-1 binds to multiple proteins that can be potential targets for therapeutics, including tissue-plasminogen activator (tPA/PLAT), urokinase-plasminogen activator (uPA/PLAU), vitronectin (VTN), and the low density lipoprotein (LDL) receptor-related protein 1 (LRP1) ⁵. When bound to tPA or uPA, PAI-1 forms a complex that renders them catalytically inactive to inhibit the conversion of plasminogen to plasmin and hence dysregulate fibrinolysis and MMP activation ⁶. Vitronectin binding to PAI-1 results in conformational changes to both proteins that lead to inhibition of vitronectin-integrin-mediated cell attachment and the stabilization of PAI-1's active conformation to amplify its inhibitory

effects on tPA/uPA ⁷. LRP1 binding to PAI-1 has reported effects on cell signaling and migration. Furthermore, LRP1 binding to PAI-1-uPAR (receptor for uPA) complex contributes to internalization and downregulation of PAI-1 ⁸. PAI-1 is also a component of the senescence-associated secretory phenotype (SASP) and can exert both paracrine and autocrine effects on cell signaling and migration, as well as on regenerative or disease conditions including wound healing, fibrosis, and cancer ⁶.

The mechanisms through which PAI-1 specifically modulates fibrosis are complex. They include inhibitory effects on matrix remodeling ^{2; 5; 6}, proinflammatory effects including macrophage activation and infiltration ⁹, possibly in association with cellular senescence as a precipitating factor ⁶, and epithelial/endothelial-to-mesenchymal transition (EMT) ⁴. Regardless of the mechanism, a variety of small molecule inhibitors of PAI-1 have been developed and investigated, with the majority of these inhibitors either targeting the PAI-1 binding domain to tPA/uPA or designed to induce a conformational change in PAI-1 to convert it to its latent form ⁵. To date, none of these inhibitors has demonstrated efficacy against the stable form of PAI-1 when bound to vitronectin, which limited their therapeutic value.

In this study, we explored pathways that are specifically activated or inhibited in a genetic model of PAI-1 deficiency, which could identify novel, less recalcitrant targets for therapy using next-generation RNA sequencing (RNA-Seq) as a powerful discovery and hypothesis-generating tool. We assessed the differential expression of genes (DEG) in purified RNA samples from mouse tendon tissues. Based on the improved tendon repair seen with global deletion of PAI-1, we characterized genes and pathways that are temporally regulated during flexor tendon healing in C57Bl/6J and PAI-1 KO mice. To obtain valuable insights into the mechanisms of fibrotic tendon healing, we defined comprehensive sets of differentially expressed genes for comparative analyses of cellular and molecular pathways and networks. Our data reveal that tendon healing involves the regulation of PI3K/Akt/mTOR, PKC, and MAPK signaling cascades, and permits consideration of these pathways for new pharmacotherapies to achieve improved tendon healing.

Methods

Animal Care and Tendon Surgery

All animal procedures were conducted in compliance with protocols approved by the University of Rochester Committee on Animal Research (UCAR). The mouse strains utilized in this study were C57Bl/6J (WT) and B6.129S2-Serpine1^{tm1Mlg/J} (PAI-1 KO) mice (Jackson Laboratory). The mouse surgery protocol involves partial laceration of the deep digital flexor tendon of the 3rd digit of the hind paw, as previously described ². Briefly, a transverse volar skin incision was made on the middle digit between the metatarsophalangeal and the proximal interphalangeal joints. The deep digital flexor tendon was separated from the two peri-located flexor digitorum superficialis tendon strips with blunt end micro-forceps. A transverse cut was made mediolaterally across roughly 50% of the width of the deep digital flexor tendon. The incision was closed using interrupted sutures (Ethicon Suture, V950G, 9-0). A sample (150 pg) of cDNA was used to generate Illumina compatible sequencing libraries with the NexteraXT library preparation kit (Illumina, San

Diego, CA) per manufacturer's protocols. The amplified libraries were hybridized to the Illumina single end flow cell and amplified using the cBot (Illumina, San Diego, CA). Single end reads of 100nt were generated for each sample.

RNA Extraction and RNA-seq

Tendon tissue (n = 3 per group) was harvested from uninjured, 2-weeks, and 4-weeks post injury tendons of WT and PAI-1 KO mice for RNA extraction and RNA-Seq analysis. Injured tendon included tissue biopsy of the healing callus, typically less than 1mm in length. Messenger RNA (mRNA) isolation and next generation RNA sequencing analysis were performed by the University of Rochester Genomics Core as described below. Briefly, tissue was flash frozen in liquid nitrogen and stored at -80°C until time of extraction. Total RNA was isolated using the RNeasy Plus Micro Kit (Qiagen, Valencia, CA) or Arcturus Pico Pure kit (Life Technologies, Carlsbad, CA) per manufacturer's recommendations. RNA concentration was determined with the NanopDrop 1000 spectrophotometer (NanoDrop, Wilmington, DE) and RNA quality assessed with the Agilent Bioanalyzer 2100 (Agilent, Santa Clara, CA).

Next Generation Sequencing (NGS) Data Processing and Alignment

Raw reads generated from the Illumina HiSeq2500 sequencer were demultiplexed using bcl2fastq version 2.19.0. Quality filtering and adapter removal are performed using Trimmomatic version 0.36 with the following parameters: "TRAILING:13 LEADING:13 ILLUMINACLIP:adapters.fasta:2:30:10 SLIDINGWINDOW:4:20 MINLEN:15" Processed/cleaned reads were then mapped to the Mus musculus reference sequence (GRCm38.p5) with STAR_2.5.2b with the following parameters: "--twopassMode Basic --runMode alignReads --genomeDir \${GENOME} --readFilesIn \${SAMPLE} --outSAMtype BAM SortedByCoordinate --outSAMstrandField intronMotif --outFilterIntronMotifs RemoveNoncanonical". Differential expression analysis and data normalization was performed using DESeq2-1.14.1 with an adjusted p-value threshold of 0.05 within an R v3.3.2 environment. Verification of differential gene expression with real-time RT-PCR was performed using TaqMan Low Density Array (TLDA) card for a select group of genes that exhibited a range of up- or down-regulation, as previously described ².

Bioinformatics and Statistical Analyses of Differentially Expressed Genes

Differential expression analysis and data normalization was performed using DESeq2-1.14.1 on RNA extracted from injured tendons at 2 and 4-weeks post injury relative to uninjured expression levels within each strain independently. Differentially expressed genes (DEG) were identified by filtering DESeq2 pairwise comparisons for biological (ABS(Log₂FC) > 1) and statistical significance (adjusted p-value < 0.05). To determine functional enrichment of signaling pathways and upstream regulators that the DEG might involve, we performed pathway enrichment analysis using Ingenuity Pathway Analysis (IPA; <http://www.ingenuity.com>). Default settings were used to determine the activation state of canonical pathways and upstream regulators using the global molecular network contained in IPA knowledge base. The activation z-score in IPA predicts the enrichment of potential pathways and regulators based on the pattern of gene regulation relevant to those pathways and regulators. Specifically, the z-score is mathematically computed by IPA to infer the

activation state of a regulator (activated vs. inhibited) and can be used to rank regulators based on statistical significance of the differential expression pattern. Downstream targets of upstream regulators identified in IPA were exported for further functional analysis using Enrichr¹⁰ (Reactome 2016 Pathways).

Data availability

The RNA-seq raw and processed data were deposited in the Gene Expression Omnibus under accession GSE125026.

Results

Differentially Expressed Genes (DEG) during Flexor Tendon Healing

The RNA integrity number (RIN) for the samples harvested for this analysis was 6.4 ± 0.97 (mean \pm standard deviation), and the RNA yield ranged from 147 to 16169 pg/ μ l. Bioinformatics analysis on DEG data from tendon tissue focused on comparisons between uninjured flexor tendons and injured tendons at 2-weeks, and 4-weeks post injury in C57Bl/6J and PAI-1 KO mice, respectively. DEG were conservatively filtered from DeSeq2 data to focus on statistically significant (adjusted p-value < 0.05) and biologically-relevant two-fold differences ($ABS(\text{Log}_2\text{Fold-Change}) > 1$) compared to uninjured tendons.

At 2-weeks post injury, 951 genes were upregulated and 668 were downregulated in C57Bl/6J injured tendon (Figure 1A - top), while 898 genes were upregulated and 878 were downregulated in the PAI-1 KO injured tendon (Figure 1A - bottom). At 4-weeks post injury, differential transcriptional regulation in C57Bl/6J injured tendon involved upregulation of 1196 genes and downregulation of 902 gene (Figure 2A - top). In contrast, 818 genes were upregulated, and 554 genes were downregulated during the healing process in the PAI-1 KO injured tendon (Figure 2A - bottom). Hierarchical clustering (Euclidean distance, ward linkage) of the DEG at 2- and 4-weeks post injury is shown in a heat map (Figure 1B and 2B).

Principal component analysis (PCA) corroborated the biological effects of the injury, healing time and the mouse genotype (Figure 3). Overall, 92% of the variance in the differential gene expression was attributed to the first three principal components (PC). Specifically, 58% of the variance was attributed to PC1, 28% to PC2, and 6% to PC3. Injured tendons clustered and clearly separated from uninjured tendons along the PC1 axis. Despite some overlap, injured tendons tended to further cluster by genotype along the PC2 axis and by healing time along the PC3 axis.

To validate DEG identified by RNA-seq, real-time RT-PCR was performed on RNA samples to quantitatively measure relative expression of a selected gene list normalized to a house keeping gene. There were strong correlations between relative expression by RT-PCR and \log_2 -fold changes by RNA-seq analysis ($R^2=0.729$; Figure 4).

Ingenuity Pathway Analysis (IPA) was subsequently performed on 6 distinct DEG lists (Figure 1C and 2C) representing genes differentially expressed in the C57Bl/6J injured tendon (827 and 1404 DEG at 2- and 4-weeks post injury, respectively), genes differentially

expressed in the PAI-1 KO injured tendon (984 and 678 DEG at 2- and 4-weeks post injury, respectively), and genes with overlapping expression in both strains (792 and 694 DEG at 2- and 4-weeks post injury, respectively).

Differentially Enriched Canonical Pathways

Enriched canonical pathways were identified by performing a core analysis in IPA with the 6 DEG lists (Figure 1 & 2). The top IPA canonical pathways positively or negatively enriched in injured tendons are represented as a z-score heat map (Figure 5). IPA predicted a substantial number of pathways that were stringently filtered herein to discuss only pathways identified for significant (adj. $p < 0.05$) activation (z-score > 2) or inhibition (z-score < -2).

At 2 weeks post injury, pathways related to ECM organization, immune system response, and cell cycle regulation were positively enriched (activated) and pathways involved in inhibition of MMPs and cell cycle checkpoint regulation were negatively enriched (inhibited) by genes expressed in both strains (Table 1). Activated Pathways in the C57Bl/6J injured tendons involved cellular immune response, cytokine signaling, the activation of actin cytoskeletal signaling, and cellular migration and infiltration (Table 2). The only activated pathway by DEG unique to the PAI-1 KO tendon was PTEN signaling (Table 3).

At 4 weeks post injury, pathways related to extracellular matrix organization (synthesis, assembly, and remodeling) and growth factor signaling in addition to persistent inflammatory response pathways were activated in both strains (Table 4). Additionally, activated pathways in the C57Bl/6J injured tendons involved innate and adaptive immune system signaling and inflammatory response pathways, in addition to mechanosignaling pathways (actin cytoskeleton and integrin) (Table 5). Inhibited pathways in the C57Bl/6J tendon involved the acute phase response signaling and the LXR/RXR activation pathway (Tables 4 and 5). On the other hand, the pathways enriched in the injured PAI-1 KO tendon at 4-weeks were the osteoarthritis pathway (activated), and EIF2 signaling (inhibited) (Table 6).

Differentially Activated or Inhibited Upstream Regulators

Numerous upstream regulators were identified to be either activated (z-score ≥ 2 , p-value of overlap < 0.05) or inhibited (z-score ≤ -2 , p-value of overlap < 0.05), which drive wide ranging biological responses associated with cytokine, growth factor, and kinase signaling, immune system responses, cell cycle regulation, cell metabolism, and extracellular matrix assembly, organization, and degradation (Tables S1 and S2). Of particular interest, activated or inhibited upstream regulators with opposing activation states in the C57Bl/6J and PAI-1 KO injured tendons were identified (Figure 6).

At 2 weeks post-injury, three upstream regulators were activated in the C57Bl/6J injured tendons, but at the same time were inhibited in the PAI-1 KO injured tendons. These include the transcription factor FOXO1, the protein kinase C (PKC) activator phorbol myristate acetate (PMA), and the pro-inflammatory protein S100A8 pathways (Figure 6-A). On the other hand, mitogen-activated protein kinase (MAPK) signaling was inhibited in the PAI-1 KO injured tendons, as indicated by enrichment of pathways related to inhibition of MAPK

signaling (PD98059 activation), with opposite effects in the C57Bl/6J injured tendons (Figure 6-A).

At 4 weeks, FOXO1 was still activated in the C57Bl/6J injured tendons and inhibited in the PAI-1 KO injured tendons. In addition, the transmembrane receptor FAS and the oncogene transcription regulator MYC were also activated in the C57Bl/6J injured tendons but inhibited in the PAI-1 KO injured tendons (Figure 6-B).

In addition, since PAI-1 is robustly induced by TGF- β 1 signaling, we examined its upstream regulatory activity. Not surprisingly, TGFB1 was a strongly enriched (activated) upstream regulator in the overlapping DEG lists at 2- and 4-weeks post injury, but with differential downstream activation of distinct biological processes in the C57Bl/6J and PAI-1 KO injured tendons DEG lists (Table 7). At 2-weeks post injury, downstream targets conserved between both strains enriched for matrix organization, deposition, and remodeling. Additionally, ECM organization enrichment was seen in the downstream targets in PAI-1 KO tendon healing as well. Interestingly, the downstream targets unique to C57Bl/6J healing were associated with cell cycle regulation and immune response. At 4-weeks post injury, TGFB1 downstream targets regulate matrix organization in all three DEG lists. However, there was continued enrichment for cytokine signaling and immune response in the C57Bl/6J tendon healing that is not observed in the PAI-1 KO tendon healing.

Discussion

Flexor tendon injuries heal imperfectly with fibrotic adhesions that limit the tissue's natural excursion function and digital joints flexion^{1; 11}. While there have been advancements in the treatment of flexor tendon injuries¹¹, these have plateaued over the past decade such that the rate of reoperation requiring tenolysis (surgical release of after primary tendon repair) still occurs in >6% of patients¹². The incomplete understanding of the complex cellular and molecular processes involved in the fibrotic healing process has hindered the development of biological therapies for scarless tendon repair. Previous findings have demonstrated that flexor tendon injuries in PAI-1 KO mice heal with reduced adhesions and accelerated recovery of biomechanical properties^{2; 13}. Due to the pleiotropic functions of PAI-1, we hypothesized that mapping whole transcriptome differences in healing flexor tendons from PAI-1-knockout mice and wildtype (C57Bl/6J) controls will reveal novel transcriptional pathways and biological drivers of the accelerated repair and reduced fibrosis. Not surprisingly, given the functional differences in the repair response between these mouse models², we found differential regulation of hundreds of genes at 2- and 4-weeks post-injury.

A nonbiased analysis of the canonical pathways enriched by the hundreds of differentially expressed genes reaffirmed the transcriptional regulation of the distinct pathways orchestrating the healing of C57Bl/6J and PAI-1 KO injured tendons. Expectedly, genes differentially-expressed in both mouse strains were involved in the enrichment of numerous canonical pathways known to regulate tissue healing including the immune system response, cell cycle regulation, and ECM organization. It is arguably more instructive to examine the pathways differentially activated or inhibited in the PAI-1 KO tendon. One such pathway,

which was activated at 2 weeks in the PAI-1 KO injured tendons only, is the PTEN pathway (Figure 7). PTEN encodes for a tumor suppressor enzyme (phosphatase and tensin homolog) that regulates cell growth (division) and death (apoptosis). PTEN is a ubiquitous negative regulator of the PI3K/Akt/mTOR and MAPK signaling pathways¹⁴. Mutations in the PTEN gene can lead to a spectrum of rare disorders known as the PTEN hamartoma tumor syndrome (PHTS)¹⁵ and have also been associated with multiple cancers¹⁶. It was recently shown that TGF- β 1-induced suppression of PTEN signaling pathway leads to fibrosis in human tenon's fibroblasts¹⁷. Analysis of alveolar epithelial cells from idiopathic pulmonary fibrosis patients also linked the activation of NF- κ B with reduced PTEN levels and both were associated with senescence, which is likely an initiating insult in lung fibrosis¹⁸. Furthermore, mTOR kinase signaling is activated downstream of PI3K/Akt in PTEN-depleted MCF7 cells¹⁹. mTOR signaling has also been associated with the onset of p53-induced cellular senescence in PTEN-deficient mouse embryonic fibroblasts¹⁹. PAI-1 has been shown to directly cause the induction of replicative senescence downstream of p53 through the activation of PI3K signaling in mouse embryonic fibroblasts⁶. Reduced PTEN signaling has been associated with renal fibrosis via p53-, smad3-, and PI3K/Akt-dependent induction of cellular senescence, which was rescued by shRNA inhibition of PAI-1²⁰. Collectively, these reports provide evidence linking PAI-1 signaling to PTEN-loss-induced cellular senescence (PICS) as a potential mediator of fibrosis. Furthermore, at 4 weeks post injury, the inhibition of the translation initiation factor EIF2 signaling pathway in PAI-1 KO tendons could also be involved in the regulation of cellular senescence through Akt-dependent responses to cellular stress²¹. Our novel observations of the transcriptional activation of PTEN signaling and inhibition of the EIF2 signaling in injured PAI-1 KO tendons, which heal with reduced fibrosis compared to the C57Bl/6J tendons², are consistent with these reports and warrant further investigation of PAI-1/PTEN modulation of cell growth or senescence in fibrotic tendon injury through PI3K/Akt/mTOR/p53 signaling.

IPA Upstream Regulator analysis predicted numerous master transcriptional regulators or biological drivers based on differential gene expression in the healing C57Bl/6J and PAI-1 KO tendons. Focusing on upstream regulators with opposing activation states in the C57Bl/6J and PAI-1 KO injured tendons reduced the expansive list and identified a few upstream regulators, which drove the enrichment of distinct biological processes in the two mouse strains. The activation of FOXO1 in the C57Bl/6J tendons at 2-weeks post-injury enriched biological processes related to regulation of different phases in cell cycle, innate and adaptive immune responses, and senescence-associated secretory phenotype (SASP). On the other hand, the inhibition of FOXO1 in the PAI-1 KO tendons at 2-weeks post-injury enriched biological pathways related to transcriptional regulation by TP53, innate and adaptive immune responses, PDGF and MAP kinase signaling, and metabolisms (Table S3). Interestingly, the enrichment of cell cycle pathways by FOXO1 activation persisted to 4-weeks post injury in the C57Bl/6J tendons, while its inhibition in the PAI-1 KO tendons at 4 weeks post injury enriched biological processes related to metabolism, homeostasis, eNOS activation, and vascular permeability (Table S4). FOXO is a family of master transcription factors that regulate diverse gene networks to determine the response of cells to stress, including cell proliferation and survival²². The activity of FOXO proteins is negatively regulated by PI3K-Akt, such that its phosphorylation by Akt inhibits FOXO nuclear

translocation and suppresses its target genes²³. FOXO1 has been reported to activate keratinocyte transition to a wound-healing phenotype, in concert with the upregulation of TGF- β 1/CTGF and their downstream targets²⁴. Others have reported that FOXO1 and FOXO3 were upregulated in skin wound healing of mice, and the partial knockout of FOXO1 in mice led to accelerated wound healing and reduced scar formation²⁵. More to the point, the activation of cardiomyofibroblasts and the onset of cardiac fibrosis in heart pathologies has been associated with noncanonical TGF- β 1 activation of FOXO transcription factors²⁶. PTEN-regulated Akt/FOXO signaling has been studied extensively in cancer²⁷ and has also been a pathway of interest in fibrosis²⁸. The observed coupling of the activation/inhibition of FOXO1- and Myc-related processes could be interesting since there are numerous reports associating Myc with the promotion of renal fibrosis²⁹, liver fibrosis³⁰, and chronic skin wounds and scarring³¹. The relationship between PAI-1 and MYC remains largely unexplored despite previous reports associating c-MYC-regulated genes with transcription of PAI-1³².

The observed transcriptional activation of the PKC signaling pathway (phorbol myristate acetate) in the C57Bl/6J injured tendons at 2 weeks, which is inhibited in the PAI-1 KO tendons, is also consistent with literature identifying multiple roles for this pathway in cell survival and apoptosis³³, senescence³⁴, and fibrosis³⁵ (Table S3). Interestingly, PKC has been shown to mediate EGFR-mTOR signaling through noncanonical pathways, and PKC inhibition led to decreased viability of glioma cells independent of PTEN or Akt³⁶. Studies have also demonstrated that PKC regulates PAI-1 through Smad6-dependent TGF- β 1 activation, and that the selective inhibition of PKC downregulates PAI-1³⁷, which could play a role in fibrotic processes in wound healing and tissue repair this mechanism has not been explored extensively.

The heterodimer S100A8/A9, also known as Calprotectin, functions primarily to promote pro-inflammatory cytokines and chemokines³⁸. When secreted, S100A8 is a damage-associated molecular pattern (DAMP) ligand for the Toll-like receptor (TLR)-4 and the receptor for advanced glycation end-products (RAGE)³⁹. As such, it plays a role in the innate adaptive immune responses to injury and has been associated with fibrosis⁴⁰, senescence⁴¹, and apoptosis⁴². The activation of FAS at this time point in the C57Bl/6J (Table S4) is also interesting and may be indicative of extrinsic cellular apoptosis⁴². Therefore, the observed activation of S100A8 as an upstream regulator in the C57Bl/6J injured tendons could be indicative of a proinflammatory etiology of fibrotic tendon healing, which appears to be transcriptionally attenuated with PAI-1 deficiency (Table S3).

Pathways related to inhibition of mitogen-activated protein kinase or MAPK (PD98059) signaling were activated in the PAI-1 KO injured tendons but inhibited in the C57Bl/6J tendons (Table S3). MAPK, also known as ERK or Extracellular signal-Regulated Kinase, can phosphorylate a variety of transcription factors including Myc and as such plays critical roles in modulating cell proliferation and cellular senescence⁴³. MAPK/ERK signaling is activated in pulmonary and renal fibrosis and its suppression has been shown to ameliorate these fibrotic pathologies⁴⁴. The upregulation of PAI-1 by TGF- β 1 has been reported to involve non-canonical (smad-independent) pathways such as MAPK activation of the transcription factor AP-1⁴⁵. Thus, the observed transcriptional inhibition of MAPK/ERK

pathway could be correlated with reduced profibrotic processes during tendon healing previously reported in the PAI-1 KO mice ^{2,46}.

TGF- β 1 is a growth factor that regulates cell proliferation, differentiation and growth, and can modulate expression and activation of other growth factors. Furthermore, TGF- β 1 is causatively associated with fibrosis due to its role in activating myofibroblasts to synthesize ECM products ⁴⁷. TGFB1 was a strongly enriched upstream regulator in multiple DEG lists but with different downstream effects in the two mouse strains, possibly indicating the role of TGF- β 1 in aberrant cell proliferation and chronic inflammation as an underlying pathology in fibrotic tendon healing in WT mice. The direct or indirect roles of PAI-1 deficiency on TGF- β 1-induced chronic inflammation in tendon healing have not been previously explored.

This study has yielded new information on molecular pathways and transcriptional upstream regulators not previously identified in tendon healing and fibrosis. However, there are limitations that qualify our conclusions. First, transcriptional profiling reflects gene expression in a mixed population of cells in the injured tissue and does not have the resolution to decipher the cross-talk between different cell types. Single cell RNA-seq analysis could mitigate this limitation, as recently described ⁴⁸. The translational relevance of these findings can be improved by cross-referencing to RNA-Seq data sets of injured human tendons. Finally, the identified pathways and biological processes were based on differential transcriptional activity in mouse tissue only and functional consequences will need to be investigated in vitro and in vivo.

In summary, this study on transcriptional profiling of tendon healing sheds new insights into the cellular and molecular mechanisms driving fibrotic tendon healing ². The study identified novel pathways that associate the fibrotic healing in flexor tendons with aberrations in cell growth and survival and chronic inflammation through complex, interrelated signaling pathways that have not been previously thoroughly explored in the context for tendon healing. These findings should motivate future studies that could lead to a better understanding of the biological limitations of natural tendon healing and the development of novel therapeutic targets to mitigate fibrosis and engineer scar-free tendon regeneration following injury.

Supplementary Material

Refer to Web version on PubMed Central for supplementary material.

Acknowledgements

The study was supported by grant numbers R01AR056696, R01AR070613, R01AR049069, and P30AR069655 from NIAMS/NIH. Funding for this work was also provided by the National Science Foundation (DMR-1206219 (DB)) and the New York State Stem Cell Science Program (NYSTEM IDEA-N11G-035, DB). MTF was supported by the Training in Orthopaedic Research Program funded by NIH T32AR053459. The content is solely the responsibility of the authors and does not necessarily represent the official views of the NIH, NSF, or NYSTEM.

References

1. Silva MJ, Boyer MI, Gelberman RH. 2002 Recent progress in flexor tendon healing. *Journal of orthopaedic science : official journal of the Japanese Orthopaedic Association* 7:508–514. [PubMed: 12181670]
2. Freeberg MAT, Farhat YM, Easa A, et al. 2018 Serpine1 Knockdown Enhances MMP Activity after Flexor Tendon Injury in Mice: Implications for Adhesions Therapy. *Sci Rep* 8:5810. [PubMed: 29643421]
3. Fortin CN, Saed GM, Diamond MP. 2015 Predisposing factors to post-operative adhesion development. *Hum Reprod Update* 21:536–551. [PubMed: 25935859]
4. Ghosh AK, Vaughan DE. 2012 PAI-1 in tissue fibrosis. *J Cell Physiol* 227:493–507. [PubMed: 21465481]
5. Placencio VR, DeClerck YA. 2015 Plasminogen Activator Inhibitor-1 in Cancer: Rationale and Insight for Future Therapeutic Testing. *Cancer Research* 75:2969–2974. [PubMed: 26180080]
6. Kortlever RM, Higgins PJ, Bernards R. 2006 Plasminogen activator inhibitor-1 is a critical downstream target of p53 in the induction of replicative senescence. *Nat Cell Biol* 8:877–884. [PubMed: 16862142]
7. Zhou A, Huntington JA, Pannu NS, et al. 2003 How vitronectin binds PAI-1 to modulate fibrinolysis and cell migration. *Nat Struct Biol* 10:541–544. [PubMed: 12808446]
8. Degryse B, Neels JG, Czekay RP, et al. 2004 The low density lipoprotein receptor-related protein is a motogenic receptor for plasminogen activator inhibitor-1. *J Biol Chem* 279:22595–22604. [PubMed: 15001579]
9. Gupta KK, Xu Z, Castellino FJ, et al. 2016 Plasminogen activator inhibitor-1 stimulates macrophage activation through Toll-like Receptor-4. *Biochem Biophys Res Commun* 477:503–508. [PubMed: 27317488]
10. Kuleshov MV, Jones MR, Rouillard AD, et al. 2016 Enrichr: a comprehensive gene set enrichment analysis web server 2016 update. *Nucleic Acids Res* 44:W90–97. [PubMed: 27141961]
11. Tang JB, Amadio PC, Boyer MI, et al. 2013 Current practice of primary flexor tendon repair: a global view. *Hand clinics* 29:179–189. [PubMed: 23660054]
12. Dy CJ, Daluiski A, Do HT, et al. 2012 The epidemiology of reoperation after flexor tendon repair. *J Hand Surg Am* 37:919–924. [PubMed: 22459656]
13. Farhat YM, Al-Maliki AA, Easa A, et al. 2015 TGF-beta1 Suppresses Plasmin and MMP Activity in Flexor Tendon Cells via PAI-1: Implications for Scarless Flexor Tendon Repair. *J Cell Physiol* 230:318–326. [PubMed: 24962629]
14. Pezzolesi MG, Platzer P, Waite KA, et al. 2008 Differential expression of PTEN-targeting microRNAs miR-19a and miR-21 in Cowden syndrome. *Am J Hum Genet* 82:1141–1149. [PubMed: 18460397]
15. Eissing M, Ripken L, Schreibelt G, et al. 2018 PTEN Hamartoma Tumor Syndrome and Immune Dysregulation. *Transl Oncol* 12:361–367. [PubMed: 30504085]
16. Naderali E, Khaki AA, Rad JS, et al. 2018 Regulation and modulation of PTEN activity. *Mol Biol Rep.*
17. Tong J, Chen F, Du W, et al. 2018 TGF-beta1 Induces Human Tenon's Fibroblasts Fibrosis via miR-200b and Its Suppression of PTEN Signaling. *Curr Eye Res.*
18. Tian Y, Li H, Qiu T, et al. 2018 Loss of PTEN induces lung fibrosis via alveolar epithelial cell senescence depending on NF-kappaB activation. *Aging Cell*:e12858. [PubMed: 30548445]
19. Jung SH, Hwang HJ, Kang D, et al. 2018 mTOR kinase leads to PTEN-loss-induced cellular senescence by phosphorylating p53. *Oncogene.*
20. Samarakoon R, Helo S, Dobberfuhl AD, et al. 2015 Loss of tumour suppressor PTEN expression in renal injury initiates SMAD3- and p53-dependent fibrotic responses. *J Pathol* 236:421–432. [PubMed: 25810340]
21. Rajesh K, Krishnamoorthy J, Kazimierczak U, et al. 2015 Phosphorylation of the translation initiation factor eIF2alpha at serine 51 determines the cell fate decisions of Akt in response to oxidative stress. *Cell Death Dis* 6:e1591. [PubMed: 25590801]

22. Poulsen RC, Carr AJ, Hulley PA. 2015 Cell proliferation is a key determinant of the outcome of FOXO3a activation. *Biochem Biophys Res Commun* 462:78–84. [PubMed: 25935481]
23. Martins R, Lithgow GJ, Link W. 2016 Long live FOXO: unraveling the role of FOXO proteins in aging and longevity. *Aging Cell* 15:196–207. [PubMed: 26643314]
24. Ponugoti B, Xu F, Zhang C, et al. 2013 FOXO1 promotes wound healing through the up-regulation of TGF-beta1 and prevention of oxidative stress. *J Cell Biol* 203:327–343. [PubMed: 24145170]
25. Mori R, Tanaka K, de Kerckhove M, et al. 2014 Reduced FOXO1 expression accelerates skin wound healing and attenuates scarring. *Am J Pathol* 184:2465–2479. [PubMed: 25010393]
26. Norambuena-Soto I, Nunez-Soto C, Sanhueza-Olivares F, et al. 2017 Transforming growth factor-beta and Forkhead box O transcription factors as cardiac fibroblast regulators. *Biosci Trends* 11:154–162. [PubMed: 28239053]
27. Hornsveld M, Dansen TB, Derksen PW, et al. 2018 Re-evaluating the role of FOXOs in cancer. *Semin Cancer Biol* 50:90–100. [PubMed: 29175105]
28. Kamo N, Ke B, Busuttill RW, et al. 2013 PTEN-mediated Akt/beta-catenin/Foxo1 signaling regulates innate immune responses in mouse liver ischemia/reperfusion injury. *Hepatology* 57:289–298. [PubMed: 22807038]
29. Shen Y, Miao N, Wang B, et al. 2017 c-Myc promotes renal fibrosis by inducing integrin alphaV-mediated transforming growth factor-beta signaling. *Kidney Int* 92:888–899. [PubMed: 28483378]
30. Nevzorova YA, Hu W, Cubero FJ, et al. 2013 Overexpression of c-myc in hepatocytes promotes activation of hepatic stellate cells and facilitates the onset of liver fibrosis. *Biochim Biophys Acta* 1832:1765–1775. [PubMed: 23770341]
31. Stojadinovic O, Brem H, Vouthounis C, et al. 2005 Molecular pathogenesis of chronic wounds: the role of beta-catenin and c-myc in the inhibition of epithelialization and wound healing. *Am J Pathol* 167:59–69. [PubMed: 15972952]
32. Prendergast GC, Diamond LE, Dahl D, et al. 1990 The c-myc-regulated gene mrl encodes plasminogen activator inhibitor 1. *Mol Cell Biol* 10:1265–1269. [PubMed: 2406566]
33. Reyland ME. 2009 Protein kinase C isoforms: Multi-functional regulators of cell life and death. *Front Biosci (Landmark Ed)* 14:2386–2399. [PubMed: 19273207]
34. Zurgil U, Ben-Ari A, Atias K, et al. 2014 PKCeta promotes senescence induced by oxidative stress and chemotherapy. *Cell Death Dis* 5:e1531. [PubMed: 25412309]
35. Song X, Qian X, Shen M, et al. 2015 Protein kinase C promotes cardiac fibrosis and heart failure by modulating galectin-3 expression. *Biochim Biophys Acta* 1853:513–521. [PubMed: 25489662]
36. Fan QW, Cheng C, Knight ZA, et al. 2009 EGFR signals to mTOR through PKC and independently of Akt in glioma. *Sci Signal* 2:ra4. [PubMed: 19176518]
37. Berg DT, Myers LJ, Richardson MA, et al. 2005 Smad6s regulates plasminogen activator inhibitor-1 through a protein kinase C-beta-dependent up-regulation of transforming growth factor-beta. *J Biol Chem* 280:14943–14947. [PubMed: 15716278]
38. Ometto F, Friso L, Astorri D, et al. 2017 Calprotectin in rheumatic diseases. *Exp Biol Med* (Maywood) 242:859–873. [PubMed: 27895095]
39. Ehlermann P, Eggers K, Bierhaus A, et al. 2006 Increased proinflammatory endothelial response to S100A8/A9 after preactivation through advanced glycation end products. *Cardiovasc Diabetol* 5:6. [PubMed: 16573830]
40. Zhang W, Lavine KJ, Epelman S, et al. 2015 Necrotic myocardial cells release damage-associated molecular patterns that provoke fibroblast activation in vitro and trigger myocardial inflammation and fibrosis in vivo. *J Am Heart Assoc* 4:e001993. [PubMed: 26037082]
41. Rashid K, Sundar IK, Gerloff J, et al. 2018 Lung cellular senescence is independent of aging in a mouse model of COPD/emphysema. *Sci Rep* 8:9023. [PubMed: 29899396]
42. Ghavami S, Kerkhoff C, Chazin WJ, et al. 2008 S100A8/9 induces cell death via a novel, RAGE-independent pathway that involves selective release of Smac/DIABLO and Omi/HtrA2. *Biochim Biophys Acta* 1783:297–311. [PubMed: 18060880]
43. Xu Y, Li N, Xiang R, et al. 2014 Emerging roles of the p38 MAPK and PI3K/AKT/mTOR pathways in oncogene-induced senescence. *Trends Biochem Sci* 39:268–276. [PubMed: 24818748]

44. Madala SK, Schmidt S, Davidson C, et al. 2012 MEK-ERK pathway modulation ameliorates pulmonary fibrosis associated with epidermal growth factor receptor activation. *Am J Respir Cell Mol Biol* 46:380–388. [PubMed: 22021337]
45. Guo B, Inoki K, Isono M, et al. 2005 MAPK/AP-1-dependent regulation of PAI-1 gene expression by TGF-beta in rat mesangial cells. *Kidney Int* 68:972–984. [PubMed: 16105028]
46. Wilde JM, Gumucio JP, Grekin JA, et al. 2016 Inhibition of p38 mitogen-activated protein kinase signaling reduces fibrosis and lipid accumulation after rotator cuff repair. *J Shoulder Elbow Surg* 25:1501–1508. [PubMed: 27068389]
47. Branton MH, Kopp JB. 1999 TGF-beta and fibrosis. *Microbes Infect* 1:1349–1365. [PubMed: 10611762]
48. Hwang B, Lee JH, Bang D. 2018 Single-cell RNA sequencing technologies and bioinformatics pipelines. *Exp Mol Med* 50:96. [PubMed: 30089861]

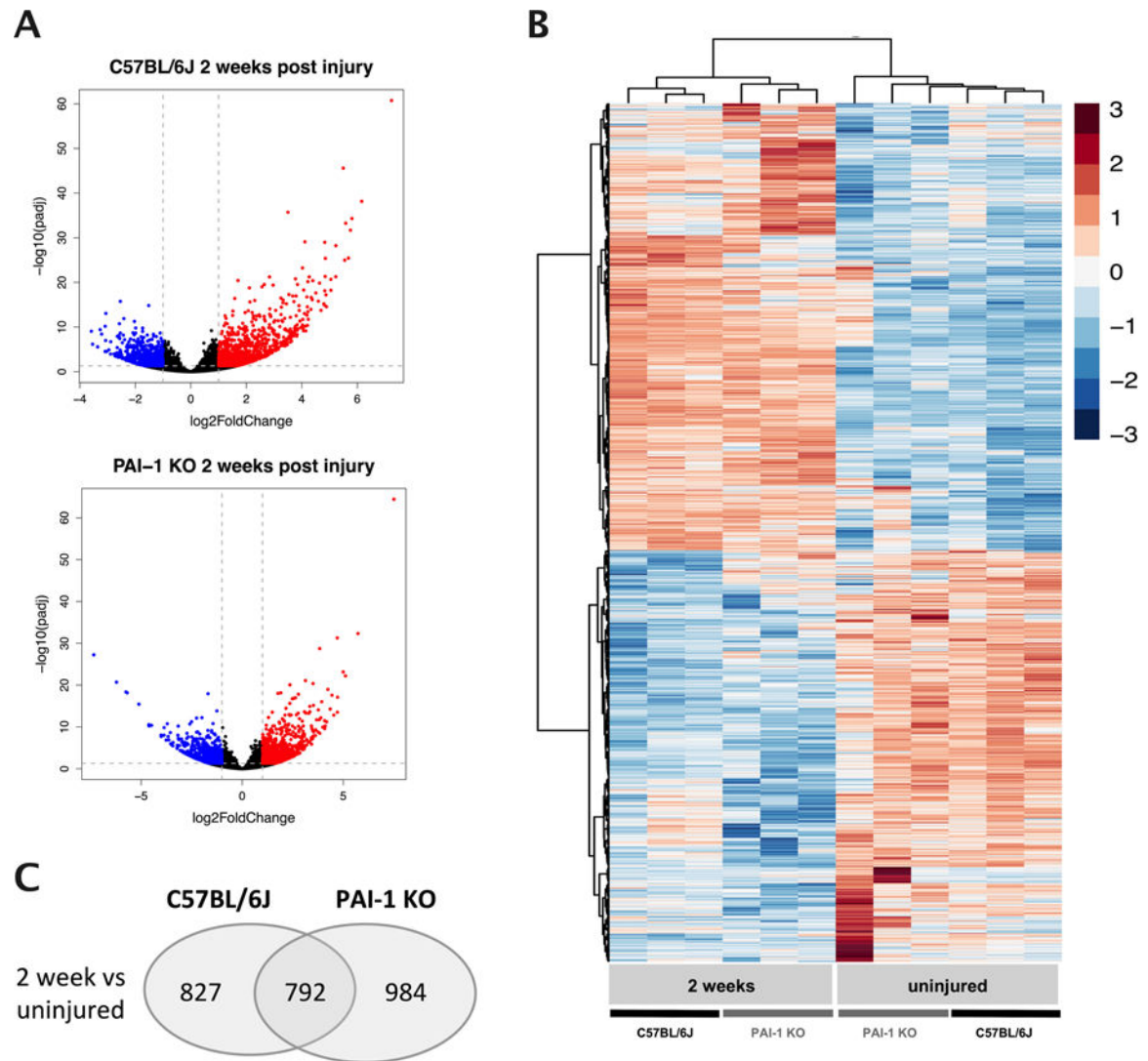


Figure 1.

RNA sequencing reveals differential and overlapping changes in gene expression during flexor tendon repair in C57BL/6J and PAI-1 KO mice at 2 weeks post-injury compared to uninjured tendons from both strains. (A) Volcano plots of differentially expressed genes at 2-weeks compared to uninjured tendon. Red dots (•) represent statistically significant, upregulated genes ($\text{Log}_2\text{FC} > 1$, $p < 0.05$). Blue dots (•) represent statistically significant downregulated genes ($\text{Log}_2\text{FC} < -1$, $p < 0.05$) in (top) C57BL/6J and (bottom) PAI-1 KO. (B) Heat map of all differentially expressed genes at 2-weeks post injury (2603 genes). Color scale based on row averages of $\text{Log}_2(\text{counts})$. Euclidian distance hierarchical clustering. (C) Venn Diagram identifying differentially expressed gene (DEG) lists. Gene lists include DEG conserved between both mouse strains (overlap) and DEG unique to each strain (C57BL/6J and PAI-1 KO).

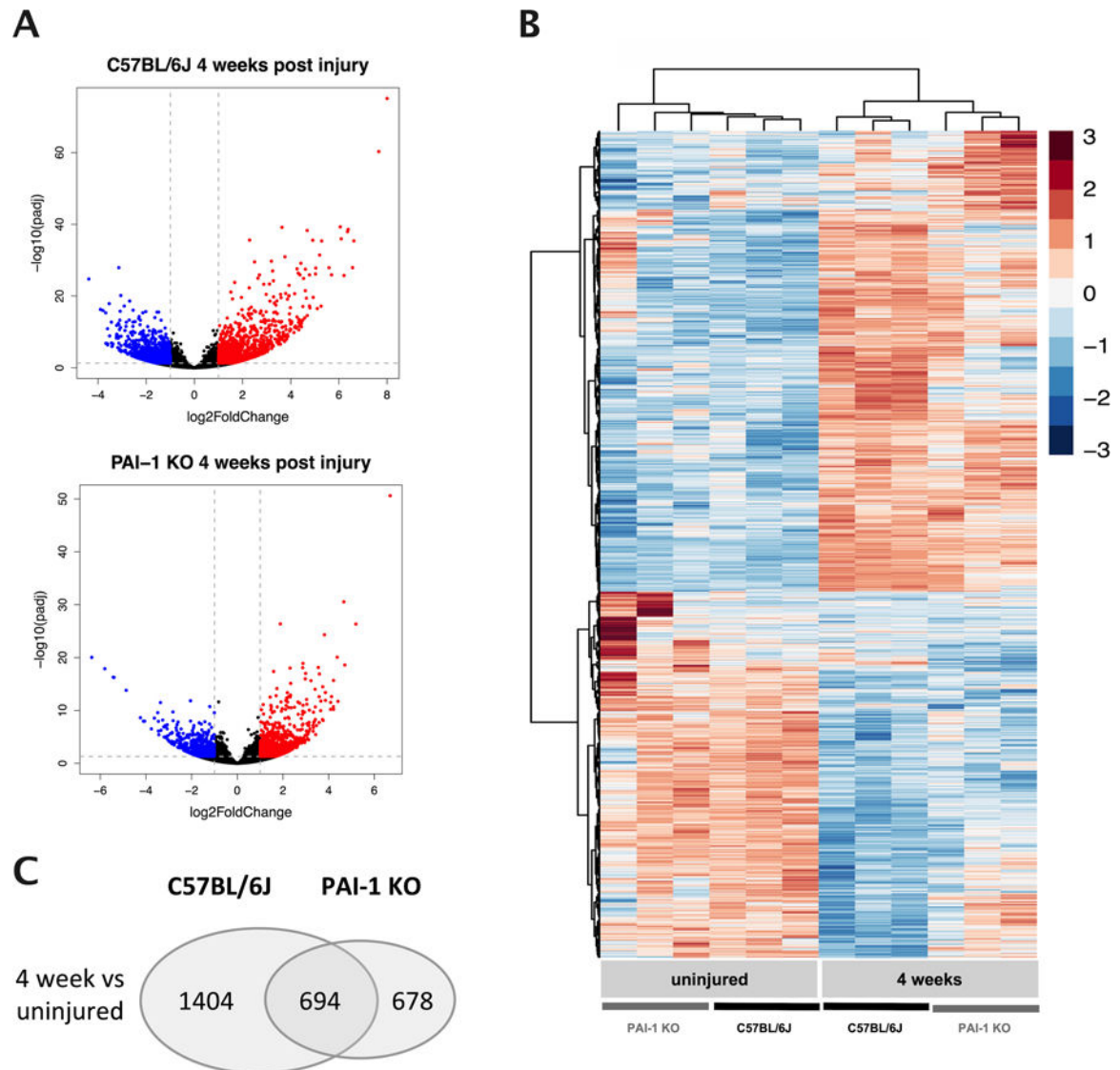


Figure 2.

RNA sequencing reveals differential and overlapping changes in gene expression during flexor tendon repair in C57BL/6J and PAI-1 KO mice at 4 weeks post-injury compared to uninjured tendons from both strains. (A) Volcano plots of differentially expressed genes at 4-weeks compared to uninjured tendon. Red dots (•) represent statistically significant, upregulated genes ($\text{Log}_2\text{FC} > 1$, $p < 0.05$). Blue dots (•) represent statistically significant downregulated genes ($\text{Log}_2\text{FC} < -1$, $p < 0.05$) in (top) C57BL/6J and (bottom) PAI-1 KO. (B) Heat map of all differentially expressed genes at 4-weeks post injury (2776 genes). Color scale based on row averages of $\text{Log}_2(\text{counts})$. Euclidian distance hierarchical clustering. (C) Venn Diagram identifying differentially expressed gene (DEG) lists. Gene lists include DEG conserved between both mouse strains (overlap) and DEG unique to each strain (C57BL/6J and PAI-1 KO).

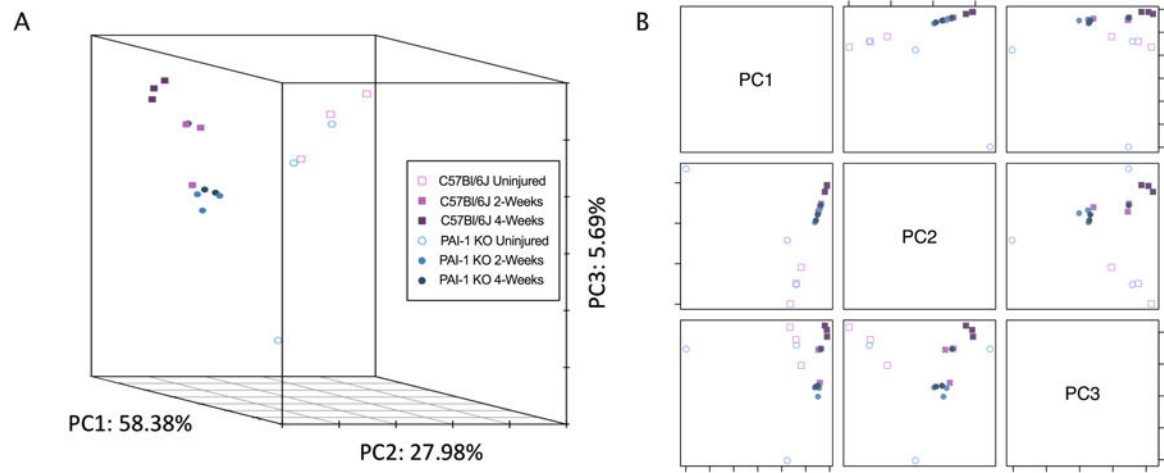


Figure 3.

Principal component analysis (PCA) of DeSeq2 Normalized Counts shown in 3D (A) and in 2D plots (B) reveals clustering of samples by injury, healing time and the mouse genotype. Injured tendons clustered along the PC1 axis and clearly separated from uninjured tendons. Despite some overlap, injured tendons further clustered by genotype along the PC2 axis and by healing time along the PC3 axis.

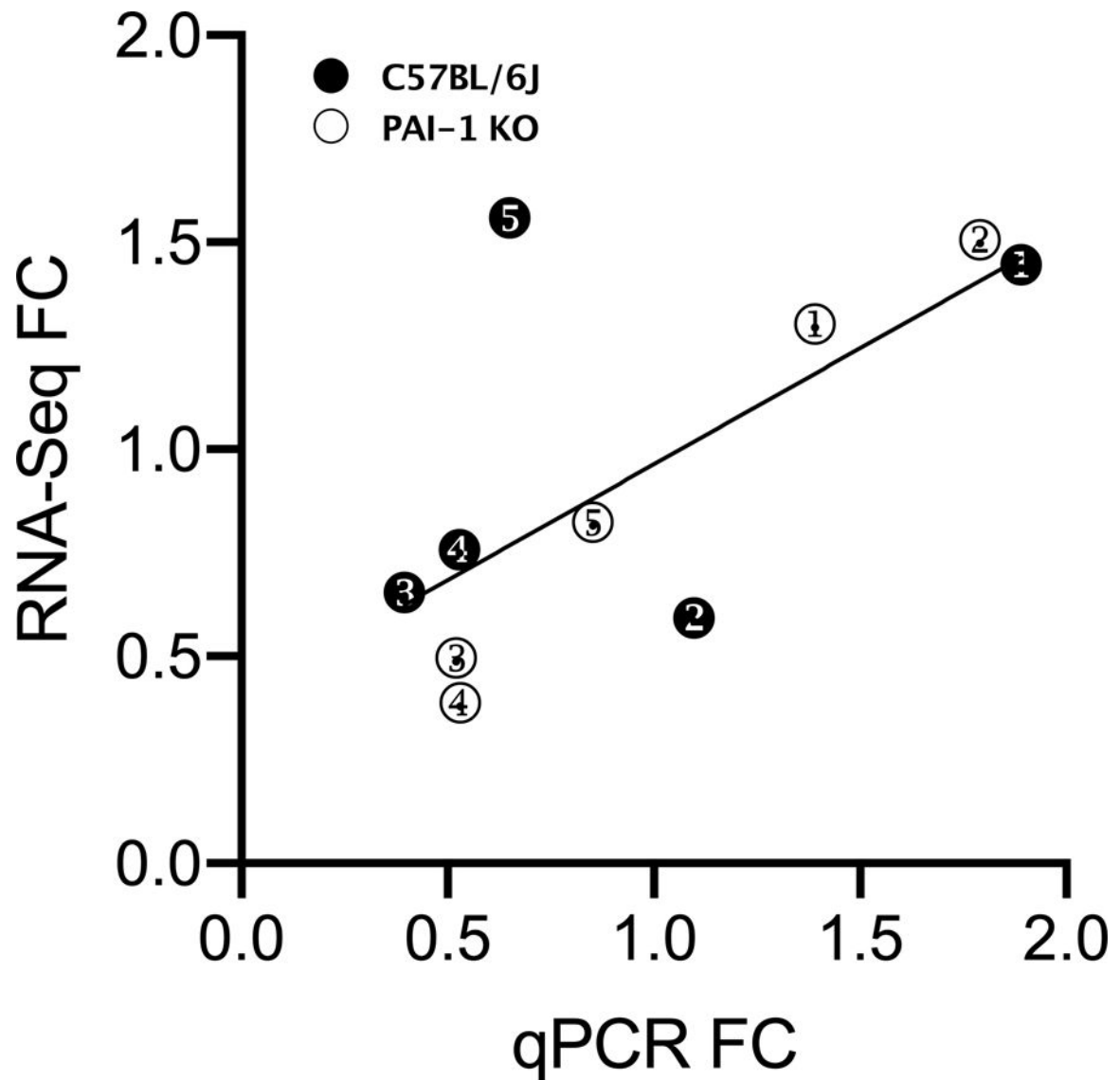


Figure 4.

RT-PCR validation of select differentially expressed genes by RNA-seq. Average Fold change (FC) determined through IPA from RNA-seq (vertical axis) were plotted against average FC determined from real-time RT-PCR measurements (horizontal axis). The genes validated were selected based on their involvement in the PI3K/Akt/mTor signaling pathway, and include (1) *Akt1*, (2) *Eif4ebp1*, (3) *Foxo1*, (4) *Mtor*, and (5) *Pten*. Correlation line represents linear regression. Fold change (FC) estimation in genes of interest in the injured tendon at 14 days-post-injury, relative to uninjured control DDFT tissue from the same genotype. Sample size n=3 per genotype per time point.

IPA Canonical Pathways

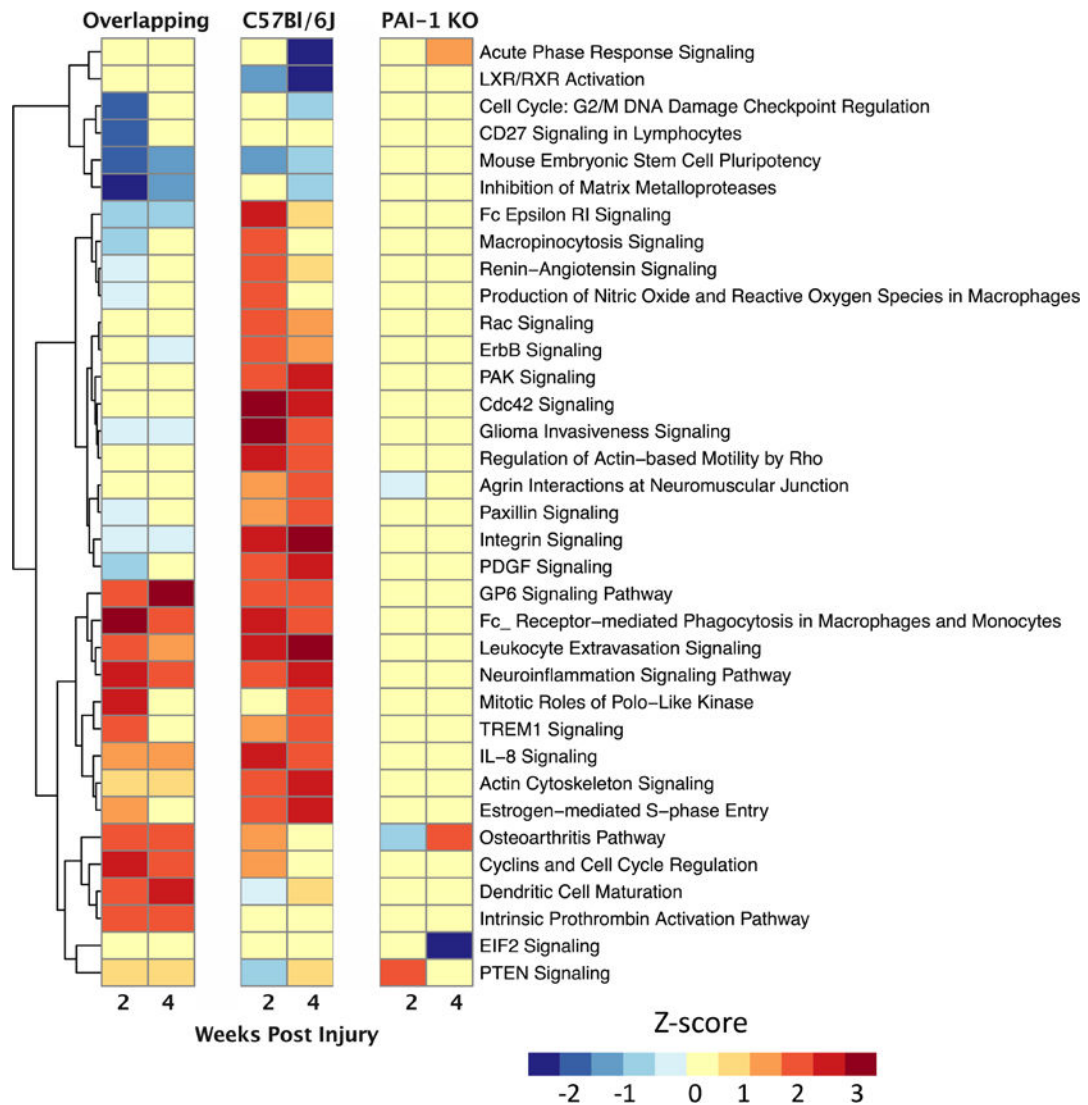


Figure 5.

Ingenuity Pathway Analysis (IPA) was used to identify top enriched canonical pathways during tendon healing. Heatmap of enriched canonical pathway that meet the threshold (to $p < 0.05$ and $ABS(z\text{-score}) > 2$) in at least one DEG analysis list. Color scale is based on activation z-score (Blue = inhibited, red = activated). Pathways are presented based on the heatmap based on Euclidian distance hierarchical clustering. The left 2 columns represent enrichment by genes in the overlapping DEG list, the middle two columns represent unique enrichment in the C57Bl/6J strain, and the right two columns represent unique enrichment in the PAI-1 KO strain at 2- and 4-weeks post injury, respectively.

A. 2-weeks post-injury

Upstream Regulator	Molecule Type	DEG List	Expr Log Ratio	Predicted Activation State	Activation z-score	p-value of overlap
FOXO1	transcription regulator	Overlap	-1.03	Activated	2.666	9.38E-09
		C57Bl/6J		Activated	2.204	4.46E-08
		PAI-1		Inhibited	-2.618	4.65E-04
Inhibition of MAPK (PD98059)	chemical - kinase inhibitor	Overlap		Inhibited	-2.169	2.95E-18
		C57Bl/6J		Inhibited	-2.171	2.00E-09
		PAI-1		Activated	2.466	9.42E-05
PKC Activation (PMA)	chemical drug	Overlap		Activated	2.724	8.42E-18
		C57		Activated	3.547	2.83E-05
		PAI-1		Inhibited	-3.847	3.71E-05
S100A8	other	Overlap	-2.767	Activated	2.132	7.93E-08
		C57Bl/6J		Activated	2.448	7.51E-05
		PAI-1		Inhibited	-2.496	1.06E-03

B. 4-weeks post-injury

Upstream Regulator	Molecule Type	DEG List	Expr Log Ratio	Predicted Activation State	Activation z-score	p-value of overlap
FAS	transmembrane receptor	C57Bl/6J	-1.108	Activated	2.718	1.75E-08
		PAI-1		Inhibited	-2.153	4.12E-04
FOXO1	transcription regulator	Overlap		Activated	2.708	6.91E-11
		C57Bl/6J		Activated	2.464	1.65E-04
		PAI-1		Inhibited	-2.5	1.00E-04
MYC	transcription regulator	C57Bl/6J		Activated	3.419	2.33E-13
		PAI-1		Inhibited	-2.095	1.83E-03

Figure 6.

Ingenuity Pathway Analysis (IPA) was used to identify activated or inhibited Upstream Regulators during tendon healing with opposing activation states in the PAI-1 KO and C57Bl/6J mice. Activation (z-score ≥ 2 , p-value of overlap < 0.05) or inhibition (z-score ≤ -2 , p-value of overlap < 0.05) was determined relative to uninjured tendon gene expression in either strain. This analysis revealed 4 differentially activated upstream regulators at 2-weeks post injury (A) and 3 differentially activated upstream regulators at 4-weeks post injury (B).

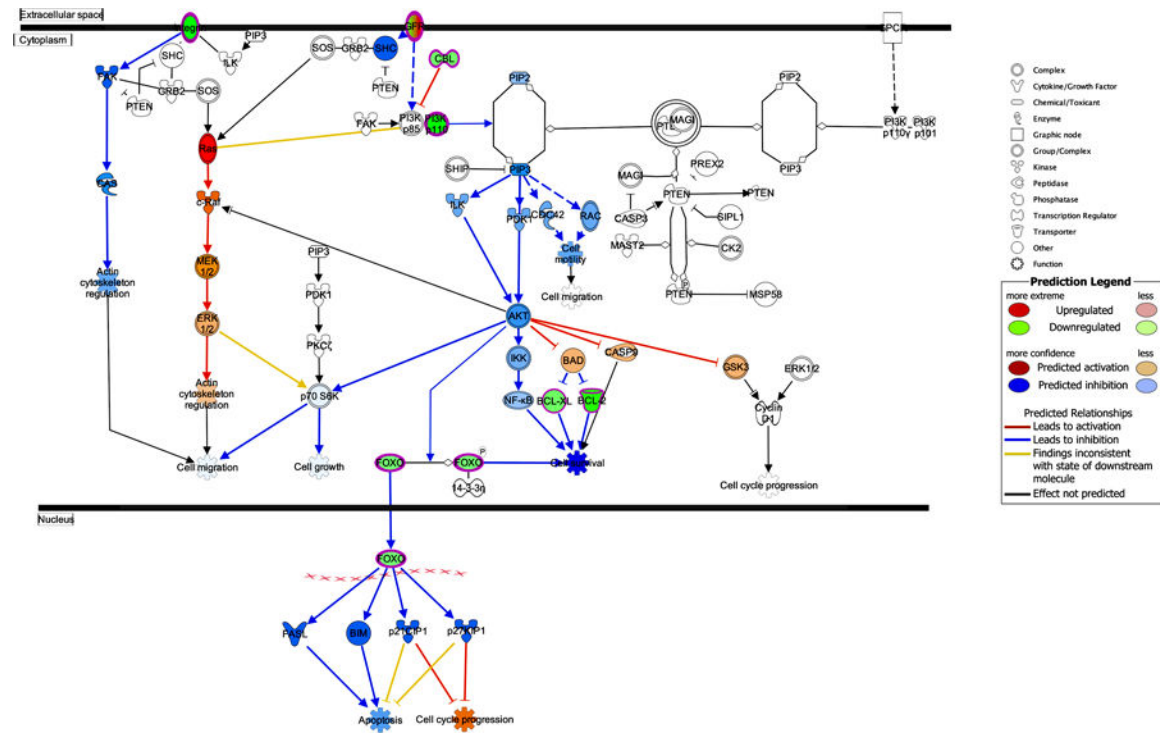


Figure 7.

Differentially expressed genes in the PAI-1 KO injured tendon that contribute to the activation of the canonical PTEN Signaling pathway at 2-weeks post injury. A total of 10 transcripts from this dataset were associated with the activation of the PTEN canonical pathway: BCL2 (−1.461), BCL2L1 (−1.106), BMPR1B (−1.324), CBL (−1.09), EGFR (1.365), FOXO1 (−1.03), ITGA2 (−2.395), PIK3CB (−1.99), RAP2B (1.583), TGFBR1 (−1.076). Numbers in parenthesis by the gene symbols indicate the expression \log_2FC (Expression False Discovery Rate (q-value) $<10^{-3}$). The cellular localization of genes in the canonical PTEN Signaling pathway was illustrated using IPA Path Designer. Red color indicates upregulated gene expression and green color represents downregulated gene expression in PAI-KO injured tendon at 2 weeks (compared with uninjured PAI-1 KO tendon). The types of molecules are annotated in the legend. The Molecule Activity Predictor (MAP) tool was used to predict *in silico* the upstream and downstream effects of these gene expression changes. Orange indicates predicted activation and blue indicates predicted inhibition.

Entrez Gene Name: BCL2 (BCL2, apoptosis regulator); BCL2L1 (BCL2 like 1); BMPR1B (bone morphogenetic protein receptor type 1B); CBL (Cbl proto-oncogene); EGFR (epidermal growth factor receptor); FOXO1 (forkhead box O1); ITGA2 (integrin subunit alpha 2); PIK3CB (phosphatidylinositol-4,5-bisphosphate 3-kinase catalytic subunit beta); RAP2B (a plasma membrane enzyme, member of RAS oncogene family); TGFBR1 (transforming growth factor beta receptor 1).

Table 1.

Conserved IPA canonical pathways in both strains at 2-weeks post flexor tendon injury

Ingenuity Canonical Pathways	−log(p-value)	Ratio	z-score	Molecules
Fcγ Receptor-mediated Phagocytosis in Macrophages and Monocytes	3.44	0.118	2.714	PLD4, HMOX1, NCF1, FCGR2A, PIK3CG, PIK3R1, HCK, RAC3, FCGR1A, FGR, VASP
Mitotic Roles of Polo-Like Kinase	2.72	0.121	2.449	CDC20, WEE1, PRC1, CCNB2, PLK1, CDK1, CHEK2, CCNB1
Cyclins and Cell Cycle Regulation	3.37	0.125	2.333	CCNA2, CCND2, WEE1, E2F7, E2F1, CDK6, TGFB2, CCNB2, CDK1, CCNB1
Neuroinflammation Signaling Pathway	6.86	0.1	2.191	MMP3, PIK3R1, TGFBR3, HLA-DQA1, CX3CR1, NGF, FGFR3, HMOX1, CCL2, HLA-DMA, PIK3CG, PLA2G5, HLA-DMB, CYBB, TGFB2, IRS2, PLA2G12B, VCAM1, CASP3, TYROBP, CD200R1, IFNGR2, BIRC5, TLR4, FOS, GAB1, TREM2, Tlr13, BACE2, S100G, HLA-DRB5
Dendritic Cell Maturation	6.6	0.119	2.132	TYROBP, FCGR2A, LEPR, PIK3R1, NFKBIE, HLA-DQA1, FCGR2B, FCGR1A, FGFR3, COL1A2, TLR4, COL1A1, PLCB4, COL5A3, GAB1, HLA-DMA, FSCN1, PIK3CG, TREM2, HLA-DMB, IRS2, HLA-DRB5, COL3A1
GP6 Signaling Pathway	6.74	0.142	2.065	COL5A2, COL6A2, COL12A1, PIK3R1, COL8A1, COL5A1, FGFR3, COL1A2, COL1A1, COL5A3, GAB1, COL6A3, COL23A1, PIK3CG, LAMB1, IRS2, KLF12, COL27A1, COL3A1
Osteoarthritis Pathway	7.03	0.118	2.041	TIMP3, FN1, CASP3, MMP3, IL1RL1, BMP2, DLX5, SMAD6, MMP10, MMP13, FZD9, HES1, CEBPB, PGF, VEGFA, FGFR3, FZD8, CASP6, TLR4, RUNX2, SIRT1, SOX9, WISP1, JAG1, ADAMTS4
Intrinsic Prothrombin Activation Pathway	2.52	0.143	2	COL1A2, KNG1, COL1A1, COL5A3, THBD, COL3A1
CD27 Signaling in Lymphocytes	1.45	0.094	−2	FOS, CASP3, MAP3K6, NFKBIE, BID
Mouse Embryonic Stem Cell Pluripotency	2.96	0.104	−2.111	LIFR, FGFR3, FZD8, ID1, BMP4, RRAS2, GAB1, PIK3CG, PIK3R1, FZD9, IRS2
Cell Cycle: G2/M DNA Damage Checkpoint Regulation	4.4	0.184	−2.121	CKS2, WEE1, TOP2A, CCNB2, PLK1, AURKA, CDK1, CHEK2, CCNB1
Inhibition of Matrix Metalloproteases	9.5	0.333	−2.887	TIMP3, MMP3, MMP14, RECK, MMP13, MMP10, MMP2, MMP23B, ADAM12, SDC2, TIMP1, MMP11, MMP19

Table 2.

IPA Canonical pathways unique to C57BL/6J flexor tendon healing at 2-weeks post injury

Ingenuity Canonical Pathways	−log(p-value)	Ratio	z-score	Molecules
Glioma Invasiveness Signaling	2.55	0.114	2.828	F2R, HMMR, CD44, PLAUR, FGFR2, PIK3CD, MMP9, ITGB3
Cdc42 Signaling	1.86	0.072	2.714	PAK1, PAK3, ARPC1B, CFL1, FCER1G, MYL4, VAV1, MYLK, HLA-DQB1, MAPK12, MAPK11, IQGAP3
Fc Epsilon RI Signaling	4.19	0.118	2.673	RAC2, FGFR2, MAPK12, MAPK11, INPP5D, PLA2G6, PLCG2, SYK, LYN, FCER1G, VAV1, PIK3CD, INPP5K, LCP2
Regulation of Actin-based Motility by Rho	1.89	0.089	2.646	RAC2, PAK1, PFN1, PAK3, ARPC1B, CFL1, MYL4, MYLK
Fcγ Receptor-mediated Phagocytosis in Macrophages and Monocytes	2.85	0.108	2.53	RAC2, PLA2G6, PAK1, TLN2, ARPC1B, SYK, LYN, VAV1, INPP5D, LCP2
IL-8 Signaling	2.43	0.076	2.324	RAC2, RELA, NOX4, VEGFC, FGFR2, HBEGF, MAPK12, CCND1, CSTB, ITGB3, ITGB2, ITGAM, NCF2, PIK3CD, MMP9
Integrin Signaling	2.38	0.073	2.324	RAC2, TSPAN5, PFN1, ARPC1B, ITGA6, FGFR2, MYLK, ITGB7, ITGB3, ITGB2, PAK1, ITGAM, TLN2, PAK3, PLCG2, PIK3CD
Leukocyte Extravasation Signaling	3.38	0.085	2.183	RAC2, MMP28, JAM2, ITGA6, FGFR2, MAPK12, MAPK11, ITGB3, TEC, ITGB2, ITGAM, ARHGAP9, PLCG2, NCF2, CD44, PIK3CD, VAV1, MMP9
Actin Cytoskeleton Signaling	3.01	0.079	2.138	RAC2, PFN1, MYH9, CFL1, ARPC1B, F2R, PDGFA, FGFR2, MYLK, PAK1, TLN2, FGF18, PAK3, MYL4, PIK3CD, VAV1, NCKAP1L, IQGAP3
PAK Signaling	2.08	0.089	2.121	PAK1, PAK3, CFL1, PDGFA, MYL4, FGFR2, MYLK, PIK3CD, MAPK12
ErbB Signaling	1.69	0.082	2.121	PAK1, PAK3, PLCG2, HBEGF, FGFR2, PIK3CD, MAPK12, MAPK11
Rac Signaling	2.6	0.094	2.111	RELA, NOX4, PAK1, PAK3, ARPC1B, CFL1, NCF2, CD44, FGFR2, PIK3CD, IQGAP3
Renin-Angiotensin Signaling	2.46	0.09	2.111	RELA, PTPN6, PAK1, PAK3, PLCG2, FGFR2, PIK3CD, CCL5, MAPK12, MAPK11, ADCY7
GP6 Signaling Pathway	2.16	0.082	2.111	COL16A1, PLCG2, SYK, LYN, FCER1G, COL22A1, FGFR2, PIK3CD, COL15A1, LCP2, ITGB3
Production of Nitric Oxide and Reactive Oxygen Species in Macrophages	1.42	0.062	2.111	RELA, PTPN6, LYZ, PLCG2, NCF2, PPP1R14A, FGFR2, PIK3CD, IRF8, MAPK12, TNFRSF1B, MAPK11
Macropinocytosis Signaling	2.71	0.111	2	MRC1, ITGB2, PAK1, PDGFA, PLCG2, FGFR2, PIK3CD, ITGB7, ITGB3

Table 3.

IPA Canonical pathways unique to PAI-1 KO flexor tendon healing at 2-weeks post injury

Ingenuity Canonical Pathways	−log(p-value)	Ratio	z-score	Molecules
PTEN Signaling	1.3	0.076	2.121	BCL2L1, CBL, TGFBR1, FOXO1, ITGA2, PIK3CB, BMPR1B, BCL2, EGFR

Table 4.

Conserved IPA canonical pathways enriched in both strains at 4-weeks post flexor tendon injury

Ingenuity Canonical Pathways	−log(p-value)	Ratio	z-score	Molecules
Leukocyte Extravasation Signaling	6.5	0.156	3.157	RAC2, MMP16, PIK3R5, MAPK11, PRKCZ, ITGB3, RASSF5, VCL, FRS2, TIMP2, ITGB1, TIMP3, CLDN10, SRC, PIK3C2B, CXCR4, MMP10, FGFR2, NCF4, MAPK12, ITGAL, PRKCG, SELPLG, TEC, PIK3R3, BTK, ITGB2, ARHGAP9, VAV3, CD44, PIK3CD, CTTN, MMP9
Integrin Signaling	3.97	0.128	3.024	RAC2, ITGA8, RHOT2, PIK3R5, MYLK, ITGB3, PAK1, ITGA11, RHOD, ITGAV, AKT3, VCL, FRS2, ITGB1, PIK3C2B, ACTR2, SRC, RRAS, FGFR2, ITGAL, PIK3R3, DOCK1, ITGB2, TLN2, PAK3, PIK3CD, CTTN, ITGAX
Neuroinflammation Signaling Pathway	5.46	0.129	2.667	RELA, TRAF3, IL12A, HLA-A, BDNF, TLR8, PIK3R5, HLA-DQA1, SLC1A3, ACVR2B, CCL5, HLA DQB1, MAPK11, TGFB2, HMOX1, IL34, AKT3, CASP8, FRS2, PIK3C2B, NOX4, NLRP3, TYROBP, CHP1, FGFR2, MAPK12, BIRC5, PRKCG, PIK3R3, PLA2G4A, CD80, SYK, S100B, Tlr13, GLUL, CD86, PIK3CD, SLC6A12, MMP9, HLA-DRB5
Cdc42 Signaling	1.68	0.102	2.53	ITGB1, SRC, ACTR2, HLA-A, HLA-DQA1, MYLK, HLA-DQB1, MAPK12, MAPK11, PRKCZ, PAK1, PAK3, EXOC5, MYL4, HLA-DRB5, HLA-E, IQGAP3
PDGF Signaling	2.61	0.144	2.496	SYNJ2, PIK3R3, PIK3C2B, SRC, RRAS, SPHK1, PIK3R5, PDGFRA, FGFR2, PIK3CD, FRS2, PDGFC, INPP5D
PAK Signaling	3.05	0.149	2.324	ITGB1, PIK3C2B, RRAS, PIK3R5, FGFR2, MYLK, MAPK12, PDGFC, PIK3R3, PAK1, PAK3, PDGFRA, MYL4, PIK3CD, FRS2
Actin Cytoskeleton Signaling	4.09	0.128	2.294	RAC2, MYH9, F2R, FGF2, PIK3R5, MYLK, SSH1, PDGFC, PAK1, FLNA, MYL4, VCL, FRS2, IQGAP3, ITGB1, ACTR2, PIK3C2B, RRAS, FGFR2, WASF1, PIK3R3, DOCK1, FGF21, TLN2, PAK3, VAV3, CD14, PIK3CD, NCKAP1L
Estrogen-mediated S-phase Entry	1.77	0.192	2.236	CCNE1, CCNE2, E2F3, CDK1, E2F8
Mitotic Roles of Polo-Like Kinase	2.28	0.152	2.121	CDC25B, KIF23, CDC25C, CDC20, PRC1, PLK1, CDK1, KIF11, CHEK2, CCNB1
Agrin Interactions at Neuromuscular Junction	3.16	0.174	2.111	ITGB1, RAC2, ITGB2, SRC, PAK1, PAK3, RRAS, UTRN, MAPK12, CTTN, ITGAL, ITGB3
TREM1 Signaling	2.34	0.147	2.111	ITGB1, RELA, NLRP3, TYROBP, CIITA, TLR8, CD86, Tlr13, AKT3, CD83, ITGAX
Paxillin Signaling	6.77	0.204	2	ITGB1, SRC, PIK3C2B, RRAS, ITGA8, PIK3R5, FGFR2, MAPK12, MAPK11, ITGAL, ITGB3, PIK3R3, DOCK1, ITGB2, PAK1, TLN2, PAK3, ITGA11, ITGAV, PIK3CD, VCL, FRS2, ITGAX
Glioma Invasiveness Signaling	5.6	0.229	2	TIMP3, PIK3C2B, F2R, RRAS, RHOT2, PIK3R5, FGFR2, ITGB3, PIK3R3, RHOD, ITGAV, CD44, PIK3CD, FRS2, MMP9, TIMP2
Fcγ Receptor-mediated Phagocytosis in Macrophages and Monocytes	3.97	0.172	2	SRC, ACTR2, RAC2, PRKCZ, INPP5D, PRKCG, PIK3R3, HMOX1, DOCK1, PAK1, TLN2, VAV3, SYK, HCK, AKT3, LCP2
LXR/RXR Activation	1.9	0.116	−2.333	RELA, C3, ABCG1, IL18RAP, IL1RL2, SREBF1, FASN, MYLIP, CD14, RXRA, HMGCR, CYP51A1, MMP9, CLU
Acute Phase Response Signaling	1.61	0.1	−2.496	SOCS1, RELA, C3, RRAS, NFKBIE, SERPINA3, MAPK12, MAPK11, NR3C1, CRABP1, PIK3R3, HMOX1, NFKBIA, AKT3, SOCS2, PIK3CD, CRABP2

Table 5.

IPA Canonical pathways unique to C57BL/6J flexor tendon healing at 4-weeks post injury

Ingenuity Canonical Pathways	−log(p-value)	Ratio	z-score	Molecules
Leukocyte Extravasation Signaling	6.5	0.156	3.157	RAC2, MMP16, PIK3R5, MAPK11, PRKCZ, ITGB3, RASSF5, VCL, FRS2, TIMP2, ITGB1, TIMP3, CLDN10, SRC, PIK3C2B, CXCR4, MMP10, FGFR2, NCF4, MAPK12, ITGAL, PRKCG, SELPLG, TEC, PIK3R3, BTK, ITGB2, ARHGAP9, VAV3, CD44, PIK3CD, CTTN, MMP9
Integrin Signaling	3.97	0.128	3.024	RAC2, ITGA8, RHOT2, PIK3R5, MYLK, ITGB3, PAK1, ITGA11, RHOD, ITGAV, AKT3, VCL, FRS2, ITGB1, PIK3C2B, ACTR2, SRC, RRAS, FGFR2, ITGAL, PIK3R3, DOCK1, ITGB2, TLN2, PAK3, PIK3CD, CTTN, ITGAX
Neuroinflammation Signaling Pathway	5.46	0.129	2.667	RELA, TRAF3, IL12A, HLA-A, BDNF, TLR8, PIK3R5, HLA-DQA1, SLC1A3, ACVR2B, CCL5, HLA-DQB1, MAPK11, TGFB2, HMOX1, IL34, AKT3, CASP8, FRS2, PIK3C2B, NOX4, NLRP3, TYROBP, CHP1, FGFR2, MAPK12, BIRC5, PRKCG, PIK3R3, PLA2G4A, CD80, SYK, S100B, Tlr13, GLUL, CD86, PIK3CD, SLC6A12, MMP9, HLA-DRB5
Cdc42 Signaling	1.68	0.102	2.53	ITGB1, SRC, ACTR2, HLA-A, HLA-DQA1, MYLK, HLA-DQB1, MAPK12, MAPK11, PRKCZ, PAK1, PAK3, EXOC5, MYL4, HLA-DRB5, HLA-E, IQGAP3
PDGF Signaling	2.61	0.144	2.496	SYNJ2, PIK3R3, PIK3C2B, SRC, RRAS, SPHK1, PIK3R5, PDGFRA, FGFR2, PIK3CD, FRS2, PDGFC, INPP5D
PAK Signaling	3.05	0.149	2.324	ITGB1, PIK3C2B, RRAS, PIK3R5, FGFR2, MYLK, MAPK12, PDGFC, PIK3R3, PAK1, PAK3, PDGFRA, MYL4, PIK3CD, FRS2
Actin Cytoskeleton Signaling	4.09	0.128	2.294	RAC2, MYH9, F2R, FGF2, PIK3R5, MYLK, SSH1, PDGFC, PAK1, FLNA, MYL4, VCL, FRS2, IQGAP3, ITGB1, ACTR2, PIK3C2B, RRAS, FGFR2, WASF1, PIK3R3, DOCK1, FGF21, TLN2, PAK3, VAV3, CD14, PIK3CD, NCKAP1L
Estrogen-mediated S-phase Entry	1.77	0.192	2.236	CCNE1, CCNE2, E2F3, CDK1, E2F8
Mitotic Roles of Polo-Like Kinase	2.28	0.152	2.121	CDC25B, KIF23, CDC25C, CDC20, PRC1, PLK1, CDK1, KIF11, CHEK2, CCNB1
Agrin Interactions at Neuromuscular Junction	3.16	0.174	2.111	ITGB1, RAC2, ITGB2, SRC, PAK1, PAK3, RRAS, UTRN, MAPK12, CTTN, ITGAL, ITGB3
TREM1 Signaling	2.34	0.147	2.111	ITGB1, RELA, NLRP3, TYROBP, CIITA, TLR8, CD86, Tlr13, AKT3, CD83, ITGAX
Paxillin Signaling	6.77	0.204	2	ITGB1, SRC, PIK3C2B, RRAS, ITGA8, PIK3R5, FGFR2, MAPK12, MAPK11, ITGAL, ITGB3, PIK3R3, DOCK1, ITGB2, PAK1, TLN2, PAK3, ITGA11, ITGAV, PIK3CD, VCL, FRS2, ITGAX
Glioma Invasiveness Signaling	5.6	0.229	2	TIMP3, PIK3C2B, F2R, RRAS, RHOT2, PIK3R5, FGFR2, ITGB3, PIK3R3, RHOD, ITGAV, CD44, PIK3CD, FRS2, MMP9, TIMP2
Fcγ Receptor-mediated Phagocytosis in Macrophages and Monocytes	3.97	0.172	2	SRC, ACTR2, RAC2, PRKCZ, INPP5D, PRKCG, PIK3R3, HMOX1, DOCK1, PAK1, TLN2, VAV3, SYK, HCK, AKT3, LCP2
LXR/RXR Activation	1.9	0.116	−2.333	RELA, C3, ABCG1, IL18RAP, IL1RL2, SREBF1, FASN, MYLIP, CD14, RXRA, HMGCR, CYP51A1, MMP9, CLU
Acute Phase Response Signaling	1.61	0.1	−2.496	SOCS1, RELA, C3, RRAS, NFKBIE, SERPINA3, MAPK12, MAPK11, NR3C1, CRABP1, PIK3R3, HMOX1, NFKBIA, AKT3, SOCS2, PIK3CD, CRABP2

Table 6.

IPA Canonical pathways unique to PAI-1 KO flexor tendon healing at 4-weeks post injury

Ingenuity Canonical Pathways	−log(p-value)	Ratio	z-score	Molecules
Osteoarthritis Pathway	1.83	0.057	2.121	S1PR3, BGLAP, TGFBR1, SP1, S100A9, TGFB1, SIRT1, ANKH, SOX9, S100A8, HES1, CASP7
EIF2 Signaling	6.66	0.1	−2.887	RPL11, RPL22, Rpl36a, RPS23, RPL39, RPS21, RPL26, RPL35A, RPL37A, RPS29, RPS28, RPS7, RPL35, RPS20, ACTA2, RPS26, Rpl39l, RPL37, PIK3R2, RPS12, RPL13A, RPS14

Table 7.
Downstream targets of TGFB1 in DEG gene list enrichment.

Downstream targets identified in IPA were exported and analyzed in Enrichr, Pathways (Reactome 2016).

2 weeks post-injury	
Overlap (201 genes) Z-score = 4.553 p-value = 7.23×10^{-53}	Extracellular matrix organization ($p = 1.8 \times 10^{-26}$) Collagen formation ($p = 8.2 \times 10^{-14}$) Assembly of collagen fibrils and other multimeric structures ($p = 1.2 \times 10^{-12}$) Degradation of the extracellular matrix ($p = 5.2 \times 10^{-10}$) Collagen degradation ($p = 1.5 \times 10^{-8}$) Collagen biosynthesis and modifying enzymes ($p = 6.2 \times 10^{-8}$) Activation of MMPs ($p = 6.3 \times 10^{-8}$)
C57Bl/6J (134 genes) Z-score = 1.624 p-value = 6.61×10^{-17}	Immune System ($p = 1.1 \times 10^{-8}$) Cell Cycle, Mitotic ($p = 4.9 \times 10^{-8}$) Cell Cycle ($p = 1.7 \times 10^{-7}$) Mitotic G1-G1/S phases ($p = 3.4 \times 10^{-8}$)
PAI-1 KO (116 genes) Z-score = 0.742 p-value = 3.21×10^{-7}	Extracellular Matrix Organization ($p = 3.0 \times 10^{-10}$) Non-integrin membranex10-ECM interactions ($p = 4.7 \times 10^{-10}$)
4 weeks post-injury	
Overlap (158 genes) Z-score = 6.811 p-value = 7.78×10^{-36}	ECM organization ($p = 1.3 \times 10^{-37}$) Collagen formation ($p = 2.5 \times 10^{-20}$) Assembly of collagen fibrils and other multimeric structures ($p = 2.8 \times 10^{-19}$) Degradation of the ECM ($p = 2.6 \times 10^{-14}$) Collagen biosynthesis and modifying enzymes ($p = 2.1 \times 10^{-13}$) Collagen degradation ($p = 1.4 \times 10^{-9}$) Elastic fibre formation ($p = 1.9 \times 10^{-9}$)
C57Bl/6J (229 genes) Z-score = 2.403 p-value = 8.71×10^{-30}	Signal transduction ($p = 3.7 \times 10^{-16}$) Immune System ($p = 1.9 \times 10^{-12}$) ECM Organization ($p = 3.4 \times 10^{-9}$) Adaptive Immune system ($p = 1.2 \times 10^{-7}$) RHO GTPase Effectors (1.2×10^{-7}) Cytokine Signaling in Immune system ($p = 2.7 \times 10^{-7}$)
PAI-1 KO (91 genes) Z-score = 1.971 p-value = 1.52×10^{-8}	ECM organization ($p = 2.0 \times 10^{-7}$) Elastic fiber formation ($p = 2.3 \times 10^{-4}$) Hemostasis ($p = 5.4 \times 10^{-3}$)